https://doi.org/10.5194/wes-2025-102
Preprint. Discussion started: 2 July 2025

eawe european academy of wind energy
Open Access WIND ENERGY SCIENCE DISCUSSIONS

Optimizing the Operation of Energy Islands with Predictive Nonlinear Programming - A case study based on the Princess Elisabeth Energy Island.

Useche-Arteaga Mario [1,2], Gebraad Pieter[1], Lacerda Vinicius [2], Cheah-Mane Marc [2], and Gomis-Bellmunt Oriol [2]

[1]Youwind, Barcelona, Spain
[2]Centre d'Innovació Tecnològica en Convertidors Estàtics i Accionaments, Departament d'Enginyeria Elèctrica, Universitat Politècnica de Catalunya, Barcelona, Spain.

Correspondence: Useche-Arteaga Mario (mario.useche@upc.edu)

Abstract. The concepts of Energy Islands or Energy Hubs have gained attention in Europe as a means to enhance offshore wind integration and regional energy systems. These islands can incorporate HVAC and HVDC transmission systems, battery energy storage systems (BESS), and hydrogen production, requiring advanced operational strategies to manage the inherent nonlinearities and time-dependence of their subsystems. To address these challenges, this work proposes a comprehensive framework for the optimal operation of hybrid AC/DC energy islands, addressing: (i) active and reactive power dispatch, incorporating BESS and hydrogen production; (ii) a detailed wind resource characterization based on one year of hourly data obtained using a realistic wind model with local measurements, including wake losses and turbine-level forecasts, used to define representative seasonal and spatial production patterns that inform typical operating conditions; and (iii) operational optimization of a realistic test system based on the Princess Elisabeth energy island, set up using commercial wind power planning tools and advanced forecasting software, and validated with Pyomo/Python.

1 Introduction

Offshore regions hold significant potential for wind energy generation, which has led to an accelerated development of offshore wind farms. In this context, the concept of energy islands has emerged as a powerful framework for planning and interconnecting these offshore wind projects. Energy islands offer a promising approach for the creation of a resilient and flexible power system, underpinned by regional interconnections. Their strategic positioning enables the integration of responsive technologies such as energy storage systems and green hydrogen production, which are vital for mitigating challenges often faced by renewable energy-dominated power grids. These challenges include issues related to voltage and frequency stability, curtailment, and fluctuations caused by the inherent intermittency of renewable energy sources, as well as grid constraints and the low system inertia. Furthermore, energy islands offer the flexibility needed to address these challenges, improving the overall reliability and efficiency of power systems that increasingly rely on renewable energy sources, as analyzed by Teng et al.

https://doi.org/10.5194/wes-2025-102
Preprint. Discussion started: 2 July 2025

(2019); Williams and Zhao (2023); Yang et al. (2023); Østergaard et al. (2023); Useche-Arteaga and et al. (2024); Lüth et al. (2024).

The optimal operation of energy islands is crucial for achieving efficient integration of offshore wind power while ensuring the safe operation of power systems. Since energy islands serve as multi-energy hubs that combine hybrid AC/DC power systems, energy storage, and green hydrogen production, sophisticated coordination strategies are required to ensure their optimal operation. The complexity of the optimal operation of these systems arises from the nonlinear interactions between their subsystems, fluctuating wind power availability, and the need to comply with physical and security constraints. Addressing these complexities requires detailed AC/DC grid models, accurate wind power forecasts, and advanced mathematical programming techniques to optimize performance, security, and cost-effectiveness. Consequently, an optimal operational strategy must achieve three key objectives: coordinate power flows efficiently, ensure safe system operation, and maximize energy utilization. This involves optimizing wind power plant dispatch, defining the set points for HVDC power converters, and strategically managing energy storage and hydrogen production.

The optimization of energy island operations lacks a unified methodology, primarily due to the nonlinear and non-convex nature of the power flow equations in the grid power model. These equations, which contain trigonometric terms, can be represented in polar or complex notation, influencing the choice of optimization approach. The main strategies include linear, convex, and nonlinear methods. Linearization, a straightforward approach, simplifies the relationships between voltage and current magnitudes and their angles in polar notation, enabling a linear approximation of active and reactive power, as presented in Ju et al. (2018). In the complex domain, linearization employs Wirtinger's calculus, as power flow equations lack conventional derivatives in complex numbers, as proposed by Garces (2022). Another methodology that has gained significant relevance in power system analysis is convex programming, as it ensures a global optimum and unique solution under well-defined conditions, while also guaranteeing algorithmic convergence, as analyzed by Arteaga et al. (2023). These advantages make convex programming a powerful tool for optimizing energy island operations. On the other hand, nonlinear programming (NLP), despite its high computational burden, allows for precise modeling of voltage–current relationships and active–reactive power interactions, as presented in Useche-Arteaga et al. (2024a). Recent advancements in numerical optimization algorithms and high-performance computing have improved NLP's tractability, as explained by Liu et al. (2022), allowing it to explore realistic operational scenarios.

AC-based energy islands, as studied by Useche-Arteaga et al. (2024b), have been identified as potentially cost-effective solutions for short- and medium-distance applications through the integration of storage and hydrogen production systems. However, their efficiency significantly declines in long-distance and high-power transmission scenarios due to increased power losses and voltage deviations, as analyzed in Useche-Arteaga and et al. (2024). Consequently, recent developments increasingly favor HVDC-based configurations, which offer inherent technical advantages such as reduced losses, enhanced voltage control, and flexible power flow management. Building upon these trends, hybrid AC/DC configurations have been proposed to leverage the benefits of both technologies; however, their operational coordination remains relatively underexplored. To address this gap, AC/DC Optimal Power Flow (OPF) methodologies offer a promising framework for improving the performance of hybrid grids. Prior research has demonstrated that OPF formulations can enhance system efficiency, ensure secure operation, and facilitate

https://doi.org/10.5194/wes-2025-102
Preprint. Discussion started: 2 July 2025

large-scale renewable energy integration. Addressing this gap, AC/DC Optimal Power Flow (OPF) methodologies offer a promising framework for improving the performance of hybrid AC/DC grids. Existing studies apply OPF models to improve system efficiency, ensure operational safety, and facilitate renewable energy integration. For instance, Ergun et al. (2019) introduce a convexified and linearized OPF formulation tailored for hybrid AC/DC grids, prioritizing computational tractability without compromising solution accuracy. Similarly, security-constrained OPF (SCOPF) approaches have been developed to enhance grid reliability under contingency scenarios in large-scale hybrid systems, as explained by Mohy-ud-din et al. (2024). The work by Cao and Yan (2016) further incorporates wind farm variability into AC/DC OPF models through iterative methods. Despite these advances, a critical gap persists: current methodologies lack explicit consideration of technologies central to AC/DC energy islands, such as such as HVDC systems, energy storage and green hydrogen production. This gap underscores the need for novel operational strategies that holistically address the specific challenges of AC/DC energy islands.

Therefore, this paper proposes a comprehensive framework for the optimal operation of AC/DC energy islands using non-linear programming, with three key contributions: (i) the development of a detailed optimization model that integrates active and reactive power dispatch while considering BESS management and hydrogen production. The framework also leverages the reactive power capabilities of wind power plants, BESS, and HVDC systems; (ii) a detailed wind resource characterization based on one year of hourly data generated using a realistic method with local measurements from Federal Public Service Economy of Belgium (2024), including wake losses and turbine-level forecasts. This analysis identifies representative seasonal and spatial patterns used to define typical daily operating conditions; and (iii) the application of the proposed framework to a realistic test system modeled after the Princess Elisabeth Energy Island, incorporating detailed turbine layout designs for offshore wind power plants.

The remainder of this paper is organized as follows: Section 2 introduces strategies for the optimal operation of AC/DC energy islands. Section 3 presents the corresponding mathematical programming models. Section 4 is divided into three core components: (i) a description of the test system based on the Princess Elisabeth Energy Island, defined using the Youwind platform; (ii) a set of simulation scenarios designed to evaluate operational challenges in offshore energy systems, leveraging the wind power forecasting capabilities of the Youwind platform; and (iii) comprehensive numerical validations assessing system performance and the effectiveness of the proposed operational strategy under varying conditions. Finally, Section 5 draws conclusions, followed by the references.

2 General Concept and Operational Strategies of AC/DC Energy Islands

Energy islands are designed to integrate multi-energy systems by combining hybrid AC/DC grids, energy storage systems, and Power-to-X technologies, as illustrated in Fig. 1. Their general design typically employs AC technology for the export cables of wind power plants, particularly for short- to medium-distance applications. However, the vast wind energy potential in far offshore areas has driven the development of energy islands toward long-distance transmission systems. Consequently, HVDC technology has become the preferred choice for most energy island projects due to its ability to efficiently transport large-scale

https://doi.org/10.5194/wes-2025-102
Preprint. Discussion started: 2 July 2025

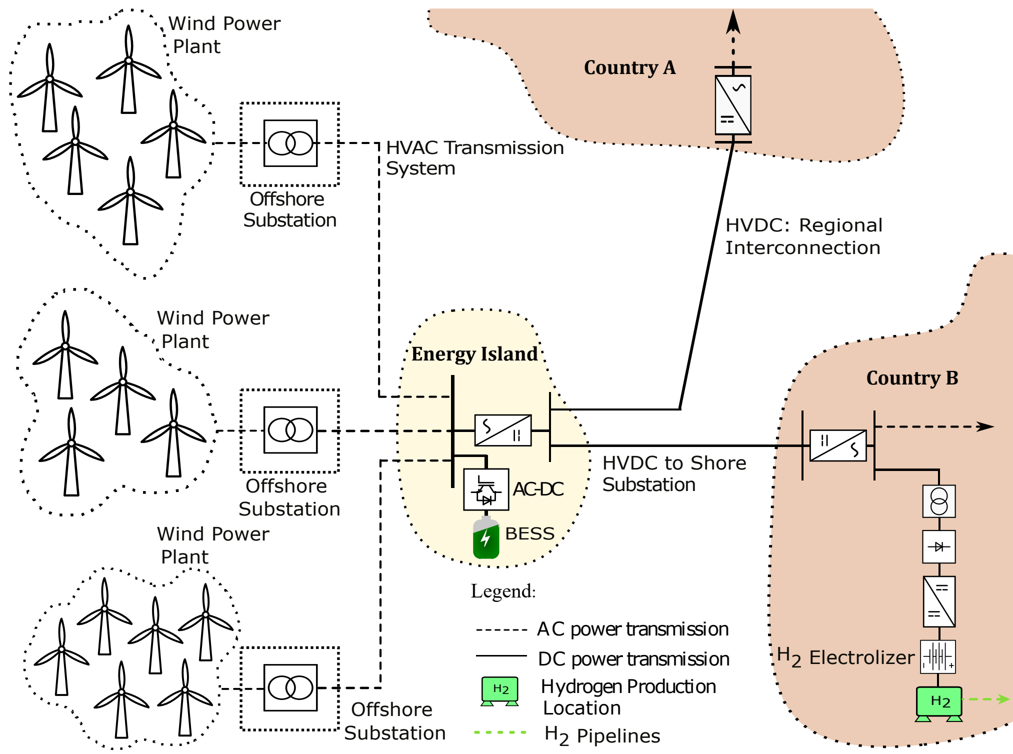

Figure 1. AC/DC Energy Island Considering Energy Storage and Hydrogen Production.

power over extended distances, meeting the operational requirements of these systems, as explained by Ansari et al. (2020); Korompili et al. (2016); Rodrigues et al. (2015).

Beyond transmission considerations, energy islands can incorporate flexible infrastructure to enhance system adaptability. For instance, energy storage systems help mitigate wind power intermittency and grid constraints. Conventional Battery Energy Storage Systems (BESS) with integrated power converters enable both active and reactive power control, reducing curtailments and supporting the reactive power needs of AC energy islands.

In addition to storage solutions, green hydrogen production plays a crucial role in energy islands. Hydrogen's high energy density makes it particularly valuable for energy-intensive industries such as steel, non-ferrous metals, and cement, as outlined by Neuwirth et al. (2022). Furthermore, as technological advancements and economies of scale drive cost reductions, hydrogen is expected to become a key player in the energy transition, as explained in the work by Ueckerdt et al. (2024). Therefore, integrating green hydrogen systems within energy islands will be essential for future power systems.

The operational strategy proposed for AC/DC energy islands adopts a centralized approach, where a central controller processes all relevant information to determine the optimal operating configuration, as illustrated in Fig. 2. The inputs to this strategy include: (i) the AC grid model, which represents the topology and electrical parameters of the array and export cables; (ii) the DC grid model, which characterizes the HVDC system interconnecting the energy island with the main grid; (iii)

https://doi.org/10.5194/wes-2025-102
Preprint. Discussion started: 2 July 2025

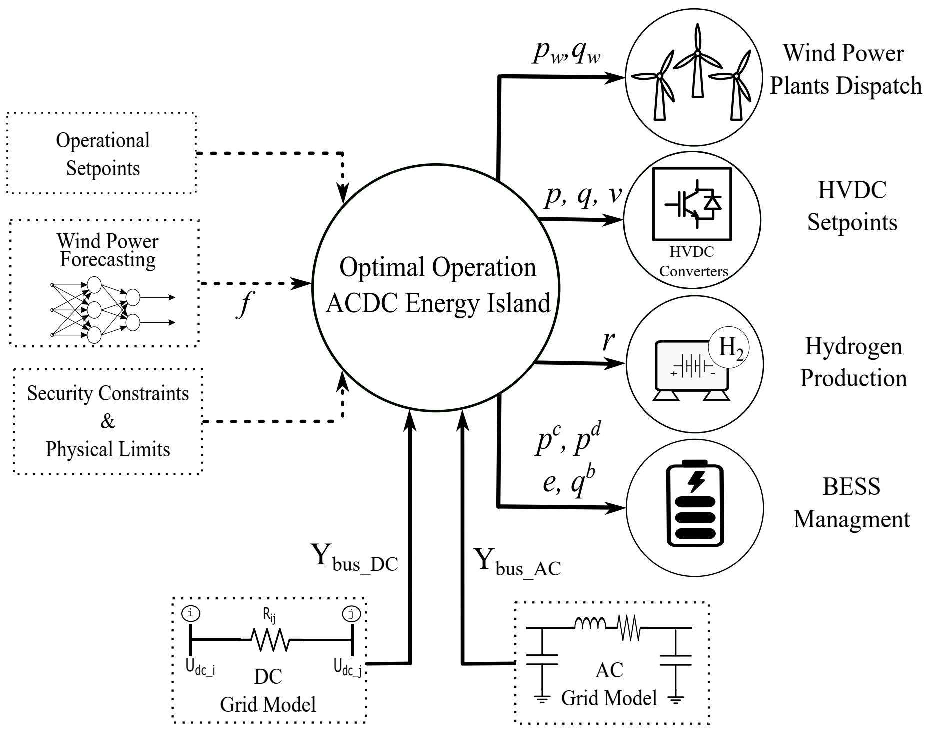

Figure 2. Diagram of the operational strategy for AC/DC energy islands.

wind power forecasts for each individual turbine within the offshore wind power plants; and (iv) the physical and security constraints required to ensure safe system operation. These constraints encompass nodal voltage limits, thermal ratings of transmission lines, and the operating limits of generators and converters within the electrical infrastructure. Additionally, operational setpoints specified by the Transmission System Operator (TSO) can be integrated into the energy management scheme to align the island's operation with system-wide requirements.

Based on these inputs, as shown in Fig. 2, the centralized controller determines the optimal operating configuration of the energy island by simultaneously coordinating: (i) the active and reactive power dispatch of the wind power plants, (ii) the setpoints of the HVDC converters, (iii) the operation of the hydrogen production system, and (iv) the management of the Battery Energy Storage System (BESS). This integrated coordination framework ensures secure and efficient operation under varying system conditions. To implement this strategy, this paper proposes a mathematical programming approach, detailed in Section 3, which optimally schedules these four subsystems within a unified decision-making model.

3 Mathematical formulation for the optimal operation of AC/DC energy islands

This study addresses the operation of AC/DC energy islands using a predictive nonlinear mathematical programming approach. Managing these complex systems requires a structured methodology to optimize decision-making while ensuring technical

https://doi.org/10.5194/wes-2025-102
Preprint. Discussion started: 2 July 2025

feasibility. The mathematical formulation of an optimization problem consists of an objective function to be maximized or minimized, subject to a set of constraints. In this context, the objective function represents the operational goals of the energy island, while the constraints ensure adherence to the physical and technical limitations of its subsystems.

The predictive component of the proposed approach is inspired by the principles of model predictive optimization, using forecasts of time-dependent operational variables, such as wind power and generation costs, over a finite horizon to guide steady-state operational decisions. By anticipating grid conditions based on these forecasts, the approach enables proactive adjustments to operation actions, ensuring optimal performance under evolving scenarios. Furthermore, the nonlinear formulation is crucial for maintaining the physical accuracy of AC/DC power flow equations, which inherently exhibit nonlinear characteristics due to the coupling of voltage magnitudes, active power, and reactive power.

This section describes the mathematical programming models for the subsystems of the AC/DC energy island, details the objective function, and presents the complete optimization problem governing its operation.

3.1 Power Grid Model

The power grid model ensures the power balance of the energy island and the conditions for the secure operation of the system, as outlined below:

3.1.1 Export and array cables of the wind power plants

The export cables refer to the export and array cables and the offshore transmission lines that connect the wind power plants to the energy island, typically using AC technology. This subsystem is modeled in the mathematical programming model using the π representation for the AC power lines, while the AC power grid is represented by the AC admittance matrix. As a result, export and array cables of the wind power plants are included in the mathematical programming model through the power balance of the AC system, as follows:

$$P_{i,t} = \nu_{i,t} \sum_{m \in \mathcal{N}_{ac}} (\nu_{m,t}[g_{im}\cos(\theta_{i,t} - \theta_{m,t}) + b_{im}\sin(\theta_{i,t} - \theta_{m,t})]), \forall i \in \mathcal{N}_{ac}, \forall t \in \mathcal{T} \quad (1)$$

$$Q_{i,t} = \nu_{i,t} \sum_{m \in \mathcal{N}_{ac}} (\nu_{m,t}[g_{im}\sin(\theta_{i,t} - \theta_{m,t}) - b_{im}\cos(\theta_{i,t} - \theta_{m,t})]) \forall i \in \mathcal{N}_{ac}, \forall t \in \mathcal{T} \quad (2)$$

Here, $\nu_{i,t}$ denotes the magnitude of the bus voltage at node i during period t, while $\theta_{i,t}$ represents the corresponding voltage phase angle. The parameters g_{im} and b_{im} correspond to the real and imaginary parts of the im-th element of the system's admittance matrix, respectively. Finally, $\mathcal{N}_{ac}$ represents the set of AC nodes in the network, and $\mathcal{T}$ is the set of periods considered within the analyzed time window.

3.1.2 HVDC Grid

The HVDC branch model for steady-state studies, such as the operation problem of energy islands, is represented by a series resistance. This HVDC branch model does not exhibit capacitive or inductive effects, which distinguishes it from HVAC

https://doi.org/10.5194/wes-2025-102
Preprint. Discussion started: 2 July 2025

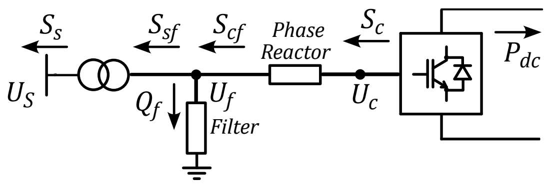

Figure 3. General Scheme of a VSC-HVDC Station

systems. This results in lower power losses, which can be considerable in comparable offshore AC transmission systems. The mathematical programming model of the HVDC grid is presented as follows:

$$P_{dc_i} = \rho \cdot u_{i,t} \sum_{\substack{j \in \mathcal{N}_{dc} \\ j \neq i}} y_{dc_{ij}} (u_{i,t} - u_{j,t}), \forall i \in \mathcal{N}_{dc}, \forall t \in \mathcal{T} \tag{3}$$

where $u_{i,t}$ represents the DC nodal voltage at node i during period t, $y_{dc_{ij}}$ denotes the DC admittance of the HVDC branch connecting nodes i and j, and ρ is a constant indicating the polarity of the HVDC branch.

3.1.3 HVDC converter station

Fig. 3 illustrates the general model of a conventional HVDC converter station, which plays a crucial role in facilitating the conversion between AC and DC power. This conversion process is essential for integrating HVDC transmission systems with AC grids. The model includes key components such as the AC filter, which mitigates harmonics and enhances power quality; the phase reactor, and the power transformer.

The AC-to-DC conversion process involves switching operations that contribute to power losses in converters. These losses depend on switching time, as power electronic devices dissipate energy during transitions between on and off states. To account for this, power losses are incorporated into the optimization model through the following constraint, where a, b and c are loss constants of the HVDC converter station, and I_c represents the converter current, as explained in the work by Valerio et al. (2025). The connection between AC and DC networks is modeled through the following power balance constraints:

$$P_{loss} = a + b \cdot I_c + c \cdot I_c^2 \tag{4}$$

$$P_{dc_i} = -P_{c_i} - P_{loss_i}, \forall i \in \mathcal{N}_{dc} \tag{5}$$

where P_{loss} represents the active power losses in the HVDC converters, modeled as a quadratic function of the converter current I_c, with a, b, and c being loss coefficients. The second equation defines the power withdrawn from the DC grid at node i, where P_{dc_i} denotes the DC power demand, P_{c_i} corresponds to the converter's output power, and P_{loss_i} accounts for the losses at node i. The set $\mathcal{N}_{dc}$ includes all DC nodes in the system.

https://doi.org/10.5194/wes-2025-102
Preprint. Discussion started: 2 July 2025

The power flow equations for the elements of the HVDC converter station, as depicted in Fig. 3, are given by

$$P_s = -U_s^2 G_{tf} + U_s U_f \big(G_{tf}\cos(\delta_s-\delta_f) + B_{tf}\sin(\delta_s-\delta_f)\big), \tag{6}$$

$$Q_s = U_s^2 B_{tf} + U_s U_f \big(G_{tf}\sin(\delta_s-\delta_f) - B_{tf}\cos(\delta_s-\delta_f)\big), \tag{7}$$

$$P_c = U_c^2 G_c - U_f U_c \big(G_c\cos(\delta_f-\delta_c) - B_c\sin(\delta_f-\delta_c)\big), \tag{8}$$

$$Q_c = -U_c^2 B_c + U_f U_c \big(G_c\sin(\delta_f-\delta_c) + B_c\cos(\delta_f-\delta_c)\big), \tag{9}$$

$$Q_f = -U_f^2 B_f, \tag{10}$$

$$P_{sf} = U_f^2 G_{tf} - U_f U_s \big(G_{tf}\cos(\delta_s-\delta_f) - B_{tf}\sin(\delta_s-\delta_f)\big), \tag{11}$$

$$Q_{sf} = -U_f^2 B_{tf} + U_f U_s \big(G_{tf}\sin(\delta_s-\delta_f) + B_{tf}\cos(\delta_s-\delta_f)\big), \tag{12}$$

$$P_{cf} = -U_f^2 G_c - U_f U_c \big(G_c\cos(\delta_f-\delta_c) + B_c\sin(\delta_f-\delta_c)\big), \tag{13}$$

$$Q_{cf} = U_f^2 B_c + U_f U_c \big(G_c\sin(\delta_f-\delta_c) - B_c\cos(\delta_f-\delta_c)\big). \tag{14}$$

Here, P_s and Q_s represent the active and reactive power at the grid side, while P_c and Q_c correspond to the active and reactive power at the converter side, respectively. The reactive power at the filter, denoted as Q_f, depends on the filter susceptance B_f. The power transfer through the transformer is characterized by P_{sf} and Q_{sf}, whereas P_{cf} and Q_{cf} describe the power flow through the phase reactor. The parameters G_{tf} and B_{tf} define the transformer conductance and susceptance, respectively, while G_c and B_c account for the phase reactor parameters. The voltage magnitudes and angles at different points of the converter station are given by U_s, U_f, U_c and $\delta_s, \delta_f, \delta_c$, as shown in Fig. 3.

3.2 Security Constraints and Physical Limits

The mathematical programming model for operating energy islands must account for constraints related to both the physical limits of power grid components and operational limits to ensure safe system operation. Specifically, the proposed model includes the constraints for the thermal limits of HVDC lines (17)-(18), thermal restrictions for AC lines (15)-(16), (19) for the power limits of the converters, constraints (20) for AC nodal voltages, and constraint (21) for DC nodal voltages.

$$\|\nu_{i,t}[y_{ij}(\nu_{i,t}-\nu_{j,t})]^*\| \le S_{ij}^{max}, \forall ij \in \mathcal{L}_{ac},, \forall t \in \mathcal{T} \tag{15}$$

$$\|\nu_{j,t}[y_{km}(\nu_{j,t}-\nu_{i,t})]^*\| \le S_{ij}^{max}, \forall ij \in \mathcal{L}_{ac},, \forall t \in \mathcal{T} \tag{16}$$

$$\|\rho u_{i,t} y_{ij}(u_{i,t}-u_{j,t})\| \le P_{ij}^{\max}, \forall ij \in \mathcal{L}_{dc}, \forall t \in \mathcal{T} \tag{17}$$

$$\|\rho u_{j,t} y_{ij}(u_{j,t}-u_{i,t})\| \le P_{ij}^{\max}, \forall ij \in \mathcal{L}_{dc}, \forall t \in \mathcal{T} \tag{18}$$

$$\|s_{c,t}\| \le s_c^{max}, \;\; s_{c,t} = p_{c,t} + jq_{c,t}, \forall t \in \mathcal{T} \tag{19}$$

$$V_{ac}^{min} \le \|\nu_{i,t}\| \le V_{ac}^{max}, \forall i \in \mathcal{N}_{ac}, \forall t \in \mathcal{T} \tag{20}$$

$$U_{dc}^{min} \le u_{i,t} \le U_{dc}^{max}, \forall i \in \mathcal{N}_{dc}, \forall t \in \mathcal{T} \tag{21}$$

https://doi.org/10.5194/wes-2025-102
Preprint. Discussion started: 2 July 2025

Here, constraints (15) and (16) ensure that the apparent power flow through AC transmission lines does not exceed the thermal limits imposed by their capacity, denoted as S_{ij}^{max}. Similarly, constraints (17) and (18) enforce the maximum permissible power transfer on DC transmission lines, defined by $P_{ij}^{\max}$. The converter operational limits are enforced by (19), which constrains the apparent power $s_{c,t}$ within the converter's rated capacity s_c^{max}. Voltage magnitude constraints for AC and DC nodes are imposed by (20) and (21), ensuring that nodal voltages remain within the prescribed operational limits V_{ac}^{min},V_{ac}^{max} and U_{dc}^{min},U_{dc}^{max}, respectively.

The proposed strategy for AC/DC energy islands includes active power dispatch of wind farms, constrained by wind power availability. Forecast wind power values are integrated into the model through constraints (22). Additionally, wind turbines can contribute to reactive power support, which is particularly relevant in offshore AC applications. The proposed approach accounts for this by incorporating reactive power dispatch. This capability is modeled by including the turbine's capability curve, which is approximated by limiting the wind turbine's apparent power to its maximum value, as defined in constraint (22).

$$\Re\left(s_{i,t}^{w}\right) \leq f_{i,t} \cdot P_{i,nom}^{w}, \forall t \in \mathcal{T} \tag{22}$$

$$\|s_{i,t}^{w}\| \leq s_{i,max}^{w}, \quad s_{i,t}^{w} = p_{i,t}^{w} + jq_{i,t}^{w}, \forall t \in \mathcal{T} \tag{23}$$

where $s_{i,t}^{w} \in \mathbb{C}$ represents the complex power generated by the wind turbine i at period t, with $p_{i,t}^{w} \in \mathbb{R}$ and $q_{i,t}^{w} \in \mathbb{R}$ denoting its active and reactive power components, respectively. The parameter $f_{i,t} \in \mathbb{R}$ corresponds to the forecasted available wind power for turbine i at time t, while $P_{i,nom}^{w} \in \mathbb{R}$ represents its nominal active power capacity. The variable $s_{i,max}^{w} \in \mathbb{R}$ defines the maximum apparent power output of the wind turbine. The notation $\Re(\cdot)$ extracts the real part of a complex number, and $\|\cdot\|$ denotes the Euclidean norm.

3.3 Battery Energy Storage System Model

Energy islands could improve flexibility by integrating energy storage systems to manage wind power intermittency, grid constraints, and curtailments. Conventional BESS, equipped with power converters, regulate both active and reactive power, minimizing curtailments while enhancing reactive power support for AC energy islands. The energy storage system is represented by constraints (24)-(29), following the linear model in Pozo (2022). This approach determines the BESS energy state using the previous state within the prediction horizon. Charging and discharging losses are incorporated through efficiency rates η^c and η^d. To ensure continuity between time windows, the initial (E_0) and final (E_f) energy states are enforced in constraint (26). This ensures that the energy state of the system is consistent and maintains a seamless transition from one time window to the next. Additionally, BESS power and storage capacity limits are imposed by constraints (27)-(29). Here, e_t represents the state of energy (SoE) of the BESS at period t, while e_{t-1} corresponds to the SoE from the previous period. The variables p_t^c and p_t^d denote the charging and discharging power of the BESS at period t, respectively. The parameters $e^{\min}$ and $e^{\max}$ define the minimum and maximum allowable SoE, while $P^{c,\max}$ and $P^{d,\max}$ impose the upper bounds on charging and discharging power.

https://doi.org/10.5194/wes-2025-102
Preprint. Discussion started: 2 July 2025

WIND ENERGY SCIENCE DISCUSSIONS

$$e_t = e_{t-1} + \eta_c P_t^c - \frac{1}{\eta_d} P_t^d, \forall t \in \mathcal{T} \tag{24}$$

$$e_{t_{ini}} = E_0 \tag{25}$$

$$e_{t_{fin}} = E_f \tag{26}$$

$$e^{\min} \leq e_t \leq e^{\max}, \forall t \in \mathcal{T} \tag{27}$$

$$0 \leq P_t^c \leq P^{c,\max}, \forall t \in \mathcal{T} \tag{28}$$

$$0 \leq P_t^d \leq P^{d,\max}, \forall t \in \mathcal{T} \tag{29}$$

Similar to wind turbines, BESS can provide reactive power support through the Q-control of their converters, enabling additional grid services. This capability is modeled as a control variable in the optimization framework to meet the reactive power demands of the AC grid. To this end, the converter's capability curve is incorporated by limiting its apparent power to the maximum allowable value, as shown in the following equations:

$$s_t^b = (p_t^d - p_t^c) + j q_t^b, \forall t \in \mathcal{T} \tag{30}$$

$$\|s_t^b\| \leq s_b^{max}, \forall t \in \mathcal{T} \tag{31}$$

where the complex power injected or absorbed by the BESS at period t is denoted as s_t^b, which consists of an active power component $(p_t^d - p_t^c)$ and a reactive power component q_t^b. Additionally, constraint (31) ensures that the apparent power of the BESS does not exceed its nominal capacity, denoted as s_b^{max}.

3.4 Green Hydrogen Production Model

Hydrogen production systems exhibit inherently nonlinear behavior, particularly in electrolyzers, where efficiency depends on factors such as voltage, current density, temperature, and degradation effects. This nonlinearity primarily stems from the electrochemical relationship between electrolyzer voltage and current density, which influences power input and hydrogen output, as explained in the work by Raheli et al. (2023). Common modeling approaches include constant efficiency, polynomial, piecewise linear, and convex approximations, as discussed by Werner (2023); Matute et al. (2021). Although constant-efficient models are widely used, such as the works by Useche-Arteaga et al. (2024a); Matute et al. (2021), they have limitations in capturing these nonlinear dynamics. To enhance accuracy, the proposed approach incorporates a linear model, formulated through the following constraints:

$$M_t = M_{t-1} + h_t, \forall t \in \mathcal{T} \tag{32}$$

$$h_t = b^h P_t^e + c^h, \forall t \in \mathcal{T} \tag{33}$$

$$M_{t_i} = \underline{M}, \forall t \in \mathcal{T} \tag{34}$$

$$M_{t_f} = \overline{M}, \forall t \in \mathcal{T} \tag{35}$$

where $h_{i,t}$ represents the hydrogen produced at node i during period t. In addition, the model considers the initial cumulative hydrogen state, M_{i,t_i}, and its final state, M_{i,t_f}, which corresponds to the hydrogen demand for the analysis period. Finally, $P_{i,t}^e$ represents the demanded power of the electrolyzer, and b_i^h and c_i^h denote the parameters of the linear model for the green hydrogen production system.

3.5 Objective function

The objective function of the proposed approach focuses on the maximization of revenue derived from offshore wind power generation. This objective reflects the importance of optimizing the economic performance of energy islands, particularly when integrating renewable energy sources such as wind power. The mathematical expression for this maximization objective function is as follows:

$$\max\ z = \sum_{t \in \mathcal{T}} \sum_{i \in \mathcal{C}} C_{i,t} P_{i,t}^m, \tag{36}$$

where $C_{i,t}$ represents the power price at country i during period t, and $P_{i,t}^m$ denotes the active power delivered to country i in period t within the time window $\mathcal{T}$.

4 Case Study: Test System Description, Simulation Scenarios, and Results

This section evaluates the proposed optimization model through a case study. It introduces the test system based on the Princess Elisabeth Energy Island, defines simulation scenarios to assess offshore operational challenges, and conducts numerical validations to analyze system performance and strategy effectiveness.

4.1 Test System Definition: Setup Based on the Princess Elisabeth Energy Island

The Princess Elisabeth Energy Island is planned for construction by the Belgian Transmission System Operator (TSO) Elia in the Belgian sector of the North Sea, approximately 45 km offshore, as described in Williams and Zhao (2023); Viaene et al. (2022); der Straeten (2022), and illustrated in Fig. 4. The energy island is designed to integrate three future offshore wind power plants: a 700 MW installation (PE-I), expected to be operational by 2028, and two additional wind power plants (PE-II and PE-III), each with a capacity of up to 1400 MW, planned for 2029, as shown in Fig. 5a.

https://doi.org/10.5194/wes-2025-102
Preprint. Discussion started: 2 July 2025

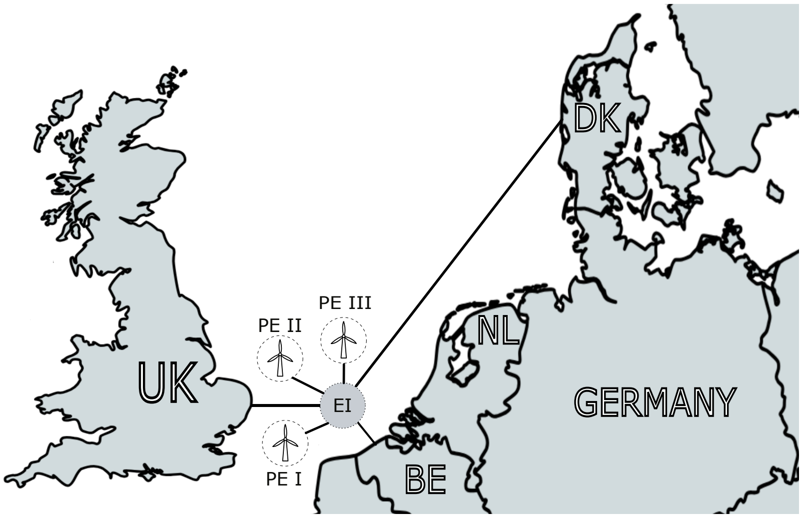

Figure 4. Test system based on the Princess Elisabeth energy island

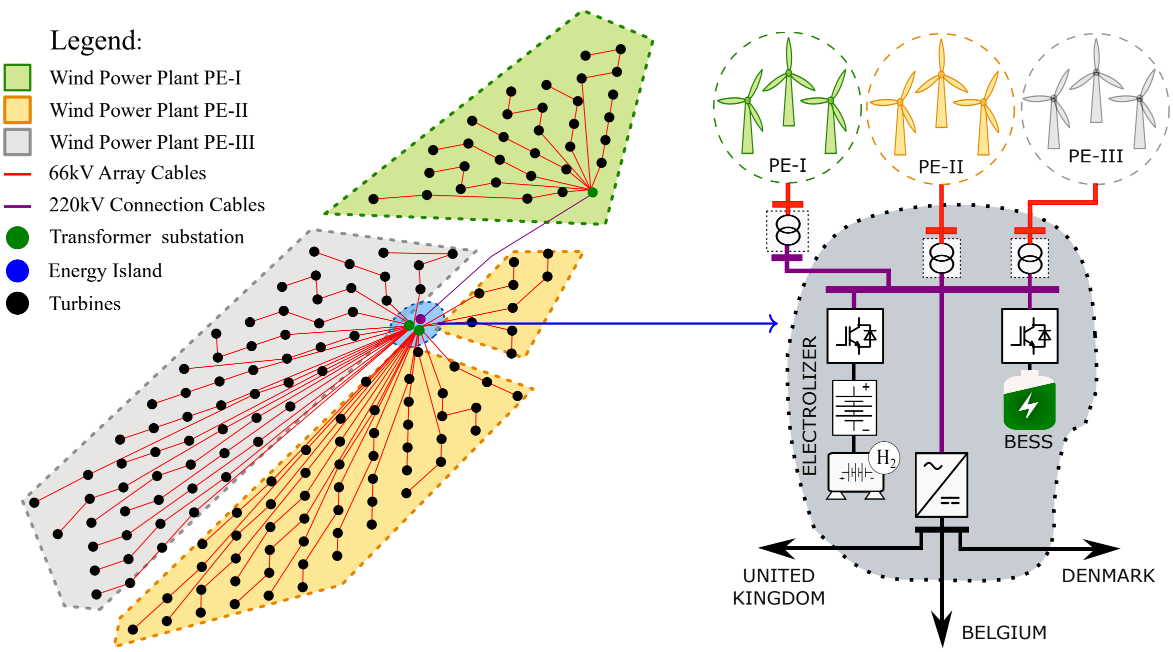

(a) Array Cable Layout of Wind Power Plants PE-I, PE-II, and PE-III.

(b) Topology of the AC/DC Energy Island with BESS and Hydrogen Production

Figure 5. AC/DC Energy Island and Grid Layout Configurations.

The infrastructure will incorporate both AC and DC technologies, where AC cables will be used for wind farm collection, while high-voltage direct current (HVDC) connections will facilitate interconnections. The HVDC links with Denmark and

https://doi.org/10.5194/wes-2025-102
Preprint. Discussion started: 2 July 2025

WIND ENERGY SCIENCE DISCUSSIONS

Table 1. Technical Parameters of BESS, Green Hydrogen Production, and HVDC Connections

Battery Energy Storage System (BESS)

Capacity [MWh]	$\underline{E}$ [MWh]	$\bar{E}$ [MWh]	$\bar{P}^c$ [MW]	$\bar{P}^d$ [MW]	η^c [%]	η^d [%]	E_0 [pu]	E_f [pu]
3500	350	3500	1155	1155	85	90	0.5	0.5

Green Hydrogen Production System

$P^e_{\max}$ [MW]	$P^e_{\min}$ [MW]	$\underline{M}_H$ [kg]	$\bar{M}_H$ [kg]	b_h [kg/MWh]	c_h [kg]
150	22.5	0	43,448	16.058	8.219

HVDC Interconnections to Onshore Grids

Parameter	Belgium	United Kingdom	Denmark
Distance [km]	40	70	600
Capacity [MW]	3500	1400	2000
Voltage [kV]	345	345	345

the UK are scheduled for commissioning in 2030. Given that these wind farms are yet to be developed, this study defines and simulates their layout within the designated areas, employing commercially available tools from Youwind (2025). Assuming full capacity utilization, the turbine layout is designed using the IEA-22 MW reference wind turbine defined in Zahle et al. (2024), applying a staggered grid arrangement with optimized row orientation and spacing to minimize wake losses, as shown in Fig. 5a. Wind Power Plant PE-I contains 32 turbines, while Wind Power Plants PE-II and PE-III contain 64 turbines.

To support the analysis, Fig. 5b presents the single-line diagram of the test system, conceptually based on the Princess Elisabeth Energy Island. The diagram illustrates the topological structure, including offshore wind farms, internal AC collection systems, HVDC converters, storage options, and export transmission links to multiple regions. This configuration serves as the foundation for simulation scenarios used to validate the proposed optimization framework. The main technical parameters are summarized in Table 1.

4.2 Hydrogen Production System: Electrolyzer model description

The Hydrogen Production System in this study was modeled in more detail and implemented in Matlab Simulink, from which measurements were obtained to identify the parameters of a linear hydrogen production model, considering both the electrical and downstream components of an electrolyzer. The electrical model is based on a voltage-current characteristic, using an empirical formula with approximated parameters for Alkaline electrolyzers from Øystein Ulleberg (2003). The downstream model links the electrolyzer current to the hydrogen production rate via chemical coefficients and Faraday efficiency, following the equations and parameters from Dozein et al. (2023). The electrolyzer stack is modeled as a series connection of cells, introducing non-linearity between consumed power and hydrogen production due to the voltage-current characteristic and Faraday efficiency effects at low current levels. Additionally, the measurements are taken on the DC side, excluding power supply losses. Finally, the parameters used for the measurements are detailed in Table 2.

https://doi.org/10.5194/wes-2025-102
Preprint. Discussion started: 2 July 2025

Table 2. Hydrogen electrolyzer nominal operating point

Parameter	**Value**
Nominal voltage	1 kV
Number of cells	455
Nominal cell voltage	2.2 V
Temperature	30 °C

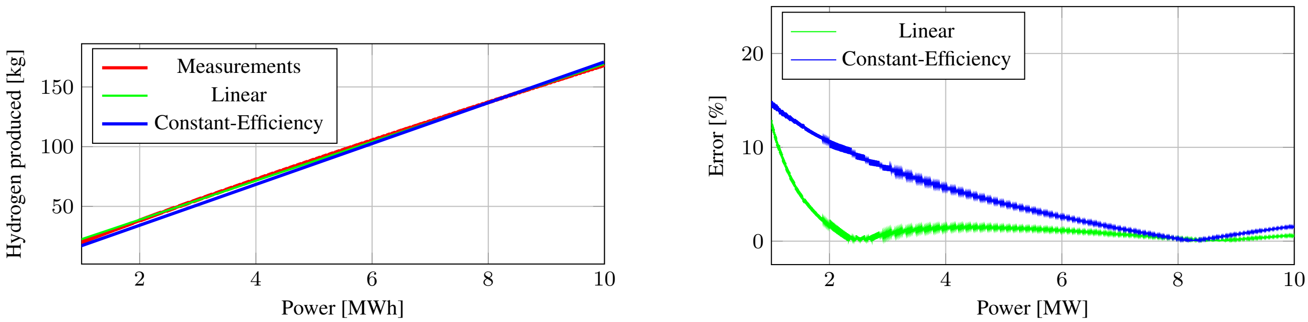

(a) Estimation of the Hydrogen Production System.

(b) Error of the Linear and Constant-Efficiency Models.

Figure 6. Results of the Hydrogen Production System estimation and model errors.

Table 3. Estimated parameters of the linear model for the hydrogen system

Parameter	**Value**	Units
b^h	16.31	kg/MWh
c^h	6.24	kg

4.3 Measurement-Based Optimization for Estimating Green Hydrogen Production Models

The efficiency of hydrogen production varies with system degradation, leading to changes in the parameters b^h, and c^h. Consequently, a significant challenge in modeling hydrogen production systems is accurately estimating the parameters of the linear model. This subsection presents a methodology for estimating the linear model for green hydrogen production systems through an optimization approach. Accordingly, the following optimization problem is proposed:

$$
\begin{aligned}
\underset{b^h,\, c^h}{\arg\min} \quad & \sum_{k=1}^{M} E_k \\
\text{s.t.} \quad & E_k = \|h_k - \tilde{h}_k\|, \\
& h_k = b^h P_k^e + c^h
\end{aligned}
\tag{37}
$$

where $\tilde{h}_k$ is the measurement of the hydrogen produced with the power P_k^e, h_k is the hydrogen production estimation based on the linear model presented in equations (32)-(35) and b^h, and c^h are the parameters estimated by the optimization problem presented in equations (37). Similarly, the parameter of the constant-efficiency model is estimated using the problem model presented in (37) with $c^h = 0$.

Fig. 6a illustrates the estimation performance of the hydrogen production system using both constant-efficiency and linear models, identified against the measured data. The associated modeling errors are presented in Fig. 6b. The linear model achieves a maximum error of approximately 12.91%, with an average and median error of 1.20% and 0.69%, respectively. In comparison, the constant-efficiency model exhibits a higher maximum error of 14.95%, along with an average and median error of 3.98% and 2.08%. These results clearly indicate the improved accuracy of the linear approach. In particular, the significantly lower mean and median errors of the linear model reflect its enhanced robustness and sensitivity in capturing variations in the input power to the hydrogen electrolyzer, making it more suitable for dynamic operational conditions.

4.4 Wind Power Profile Analysis of the Princess Elisabeth Energy Island

This subsection analyzes the wind power profiles of the three offshore wind power plants integrated into the Princess Elisabeth Energy Island. The objective is to characterize both seasonal and spatial patterns in the available power, based on hourly production data over a full year,generated using a simulation of the wake losses in the wind parks and wind speed and direction timeseries provided by the Federal Public Service Economy of Belgium (2024). These patterns are used to identify representative daily profiles for each season, which are later used to define typical operating conditions in the optimization framework. The analysis includes the statistical distribution of daily average power, representative daily curves, and turbine-level power output for a representative day.

Figure 7 shows the seasonal distribution of average daily power for each of the three wind power plants. The boxplots summarize the statistical variability of the available power across the four seasons, based on daily average values. The central line indicates the median, the box spans the interquartile range (25th to 75th percentiles), and whiskers extend to 1.5 times the interquartile range. Autumn shows the highest median daily power across all wind power plants, while Summer consistently presents the lowest. Spring and Winter exhibit intermediate values, with Winter showing greater variability. Rather than using a full year of data, we demonstrate the optimization on representative days for each season, to keep the calculation time for the study limited, while still capturing the key seasonal characteristics of offshore wind variability. Based on these analyses and the simulation of the wind parks in the Youwind platform using the N.O. Jensen wake model (Katic et al. (1987)), we obtained turbine-level power forecasts, which constitute one of the key inputs for implementing the proposed optimization approach.

Figure 8 shows the representative daily profiles of hourly wind power generation for each wind power plant: PE_I (a), PE_II (b), and PE_III (c). For each season, a representative day was selected by identifying the daily profile whose average total power was closest to the seasonal median. The curves reflect typical intraday generation behavior under seasonal wind conditions. These profiles provide seasonally realistic input scenarios for the operation of the hybrid energy island.

https://doi.org/10.5194/wes-2025-102
Preprint. Discussion started: 2 July 2025

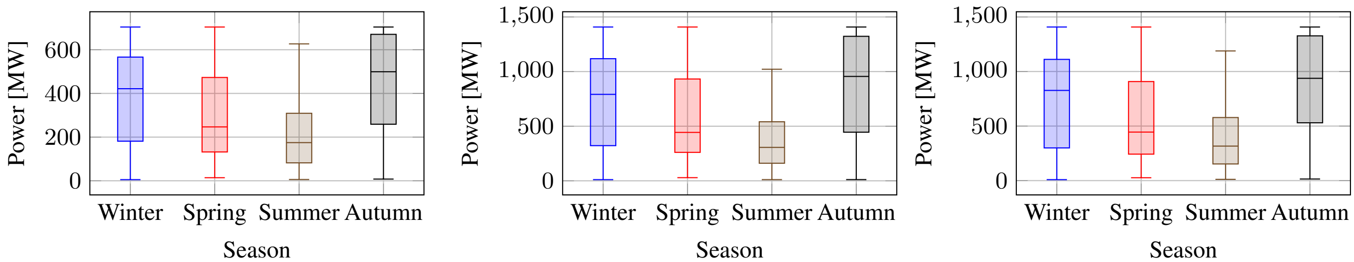

(a) PE_I (b) PE_II (c) PE_III

Figure 7. Seasonal distribution of average daily power for the three wind power plants over a year.

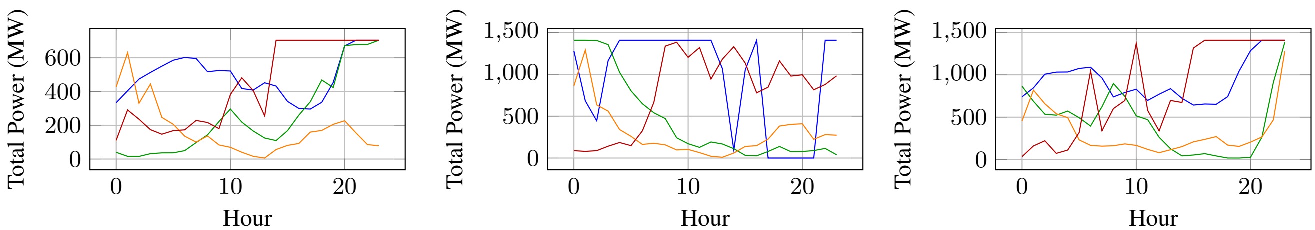

(a) PE_I (b) PE_II (c) PE_III

Figure 8. Seasonal representative daily profiles of hourly power generation for each wind power plant (PE_I, PE_II, and PE_III).

Finally, Figure 9 shows the hourly wind speed and power output per turbine in PE_I for the representative winter day. The plot illustrates the spatial variability in turbine performance over the course of a day, influenced by wake effects and wind direction, and highlights the importance of considering spatial resolution in wind power modeling.

4.5 Energy Management and Optimization for Representative Days on the Princess Elisabeth Energy Island

In this subsection, we present the results of applying a nonlinear optimization model to the operation of the Princess Elisabeth Energy Island, focusing on representative days that encapsulate typical seasonal variations in wind power availability and electricity prices.

However, before proceeding with the multiperiod and seasonal analyses, a preliminary validation of the proposed optimization approach was conducted to ensure its reliability under nominal operating conditions. Specifically, a double-check was performed using the Python-based power flow tool pyflow_acdc, developed by Valerio et al. (2025). The comparison shows that both approaches yield very similar results, with the proposed method achieving a 1.5% improvement in the objective function value compared to pyflow_acdc, thereby demonstrating the accuracy and robustness of the optimization results.

https://doi.org/10.5194/wes-2025-102
Preprint. Discussion started: 2 July 2025

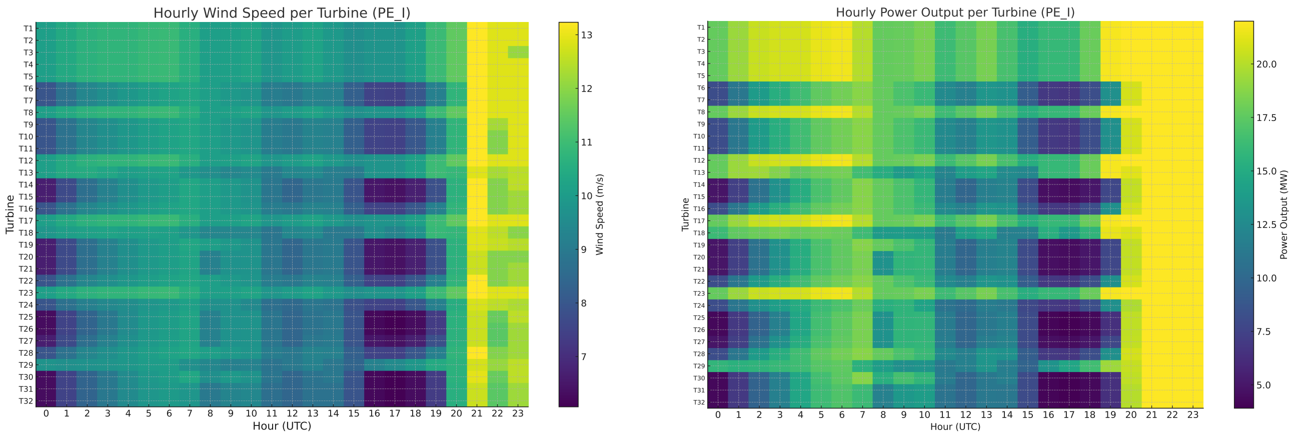

(a) Wind speed per turbine (PE_I).

(b) Power output per turbine (PE_I).

Figure 9. Hourly turbine-level wind speed and power output in PE_I on a representative winter day, illustrating spatial variability and wake effects across the wind power plant.

After validating the proposed approach, the analysis focuses on the representative days selected to characterize the seasonal operation of the energy island. Figure 8 illustrates the seasonal representative daily profiles of hourly power generation for the three wind power plants (PE_I, PE_II, and PE_III) integrated into the energy island, with each plant's profile displayed in dedicated subfigures. These profiles provide a detailed representation of wind power availability across different seasons, serving as a fundamental input for the optimization model. Complementing this, Figure 10 shows the day-ahead electricity price profiles for the representative seasonal day in the UK, Belgium, and Denmark, which are pivotal for the economic optimization of the energy island's operation. The electricity price data for Belgium and Denmark were obtained from ENTSO-E (2025), while the UK prices were sourced from Elexon (2025). Leveraging these wind power and electricity price profiles, the nonlinear model optimizes the power dispatch from the wind turbines, the charging and discharging schedules of the battery energy storage systems, and the production rates of green hydrogen, while accounting for the detailed characteristics of the energy island's AC/DC infrastructure. The results demonstrate the effectiveness of the proposed optimization framework in coordinating the energy island's resources, ensuring both operational efficiency and system reliability across diverse conditions.

To facilitate a structured analysis, the evaluation has been divided into two stages. First, we present a detailed operational analysis of a representative day for the autumn season. This focused assessment allows for an in-depth examination of the system's performance throughout a typical day under a specific seasonal scenario. Subsequently, we extend the analysis by presenting the representative daily profiles for all four seasons. This broader assessment demonstrates the capability of the proposed approach to adapt the optimal operational strategy to the varying conditions across the year.

Figure 10 presents the representative autumn daily profiles of electricity prices and dispatched power for Belgium (BE), Great Britain (GB), and Denmark (DK). The top subfigures show that electricity prices peak around 199 €/MWh at hour 10 in BE, 191 €/MWh at hour 6 in GB, and 199 €/MWh at hour 10 in DK. In response, the bottom subfigures illustrate the dispatched

https://doi.org/10.5194/wes-2025-102
Preprint. Discussion started: 2 July 2025

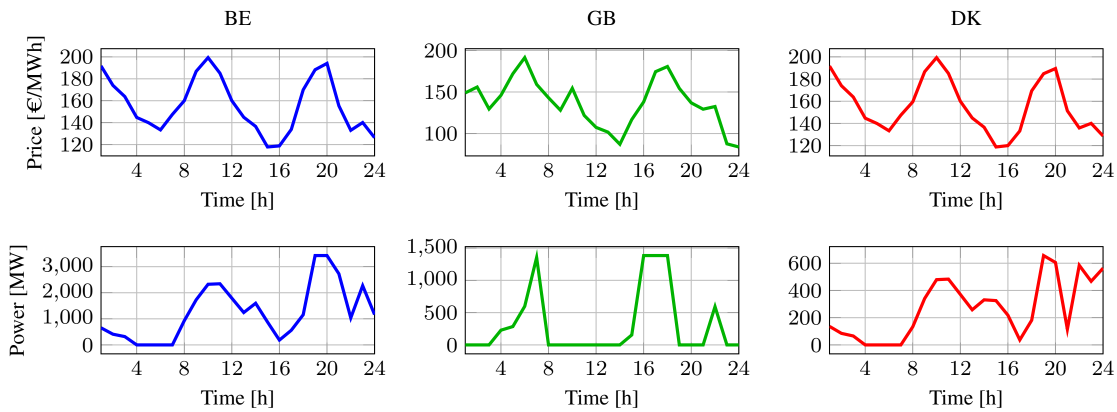

Figure 10. Representative autumn daily profiles. Top row: hourly electricity prices for Belgium (BE), Great Britain (GB), and Denmark (DK). Bottom row: dispatched power to the corresponding onshore grid in per unit [MW].

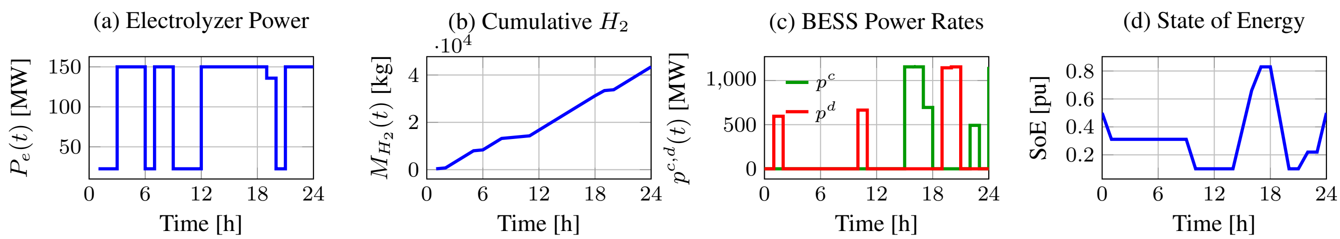

Figure 11. Operational profiles of the hydrogen production and battery storage systems during a representative autumn day: (a) Electrolyzer power $P_e(t)$, (b) cumulative hydrogen production $M_{H_2}(t)$, (c) BESS power charging/discharging rates $p^c(t)$ and $p^d(t)$, and (d) battery state of energy (SoE).

power profiles optimized according to these electricity price profiles. In BE, substantial exports occur between hours 8 and 22, with a maximum dispatch of approximately 3.43 GW at hours 19–20, coinciding with the higher electricity prices observed during these periods. In GB, exports are concentrated around hours 4–7 and 15–18, following the increases in electricity prices during the early morning and late afternoon. Despite similar price levels between BE and DK, dispatched power to DK remains lower, with peaks around 656 MW at hour 19, primarily due to the greater distance and associated transmission losses between the energy island and the Danish grid. The operation of the battery energy storage system (BESS), as illustrated in Figure 11, further enhances the dispatch strategy: the BESS charges predominantly during lower-price periods around hours 15–18 and 22–24, with charging powers up to 1155 MW, and discharges during high-price intervals, notably at hours 10 and 19–20 with discharging peaks above 1140 MW. The hydrogen production system dynamically adjusts its operation, reducing electrolyzer power to 22.5 MW at hours 10 and 19–20 to prioritize electricity exports during price peaks, while otherwise absorbing surplus renewable generation, thus guaranteeing the fulfillment of the daily hydrogen production demand, which constitutes a critical operational constraint for the energy island.

https://doi.org/10.5194/wes-2025-102
Preprint. Discussion started: 2 July 2025

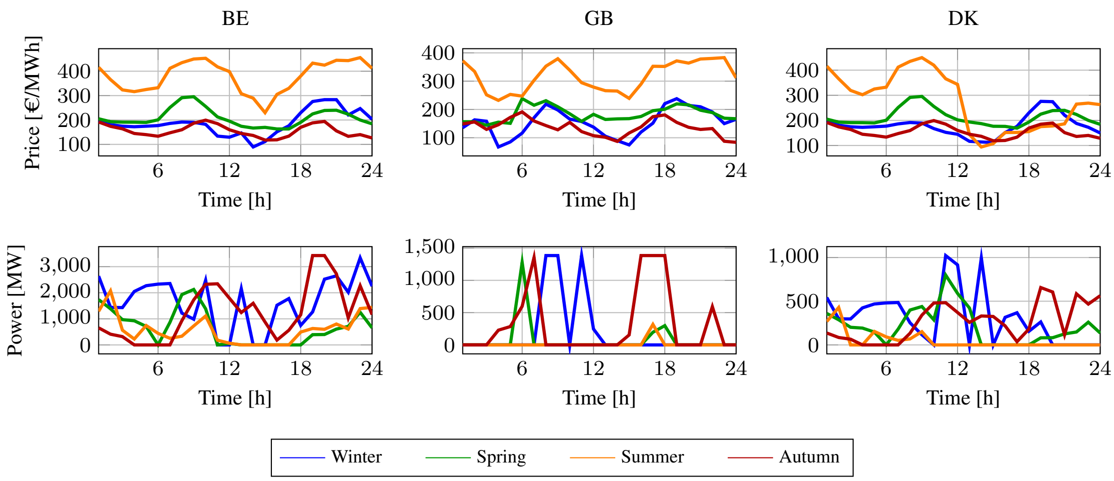

Figure 12. Hourly energy prices (top row) and dispatched power (bottom row) for Belgium (BE), Great Britain (GB), and Denmark (DK) for representative days in the four seasons.

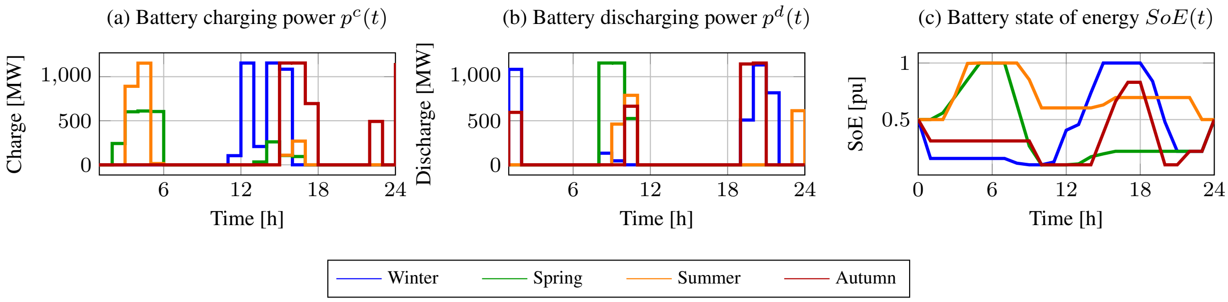

Figure 13. Seasonal variation of battery operation: (top) charging power $p^c(t)$, (middle) discharging power $p^d(t)$, and (bottom) state of energy $SoE(t)$.

Figures 12, 13, and 14 illustrate the seasonal operation of the energy island, covering the hourly electricity prices, the dispatched power to the onshore grids, and the performance of the battery and hydrogen production systems. The results clearly reflect the seasonal variability in both offshore wind generation and market prices. Despite these fluctuations, the proposed optimization framework dynamically adjusts energy dispatch, BESS management, and hydrogen production to maximize economic revenues while ensuring the secure operation of the energy island and the power system. In the representative days analyzed, the dispatched energy varies from 15,506 MWh in summer to 51,246 MWh in winter, with intermediate values of 23,018 MWh in spring and 43,971 MWh in autumn. Similarly, the revenues range from approximately €5.31 million in spring to €10.14 million in winter, with €6.27 million in summer and €7.26 million in autumn.

https://doi.org/10.5194/wes-2025-102
Preprint. Discussion started: 2 July 2025

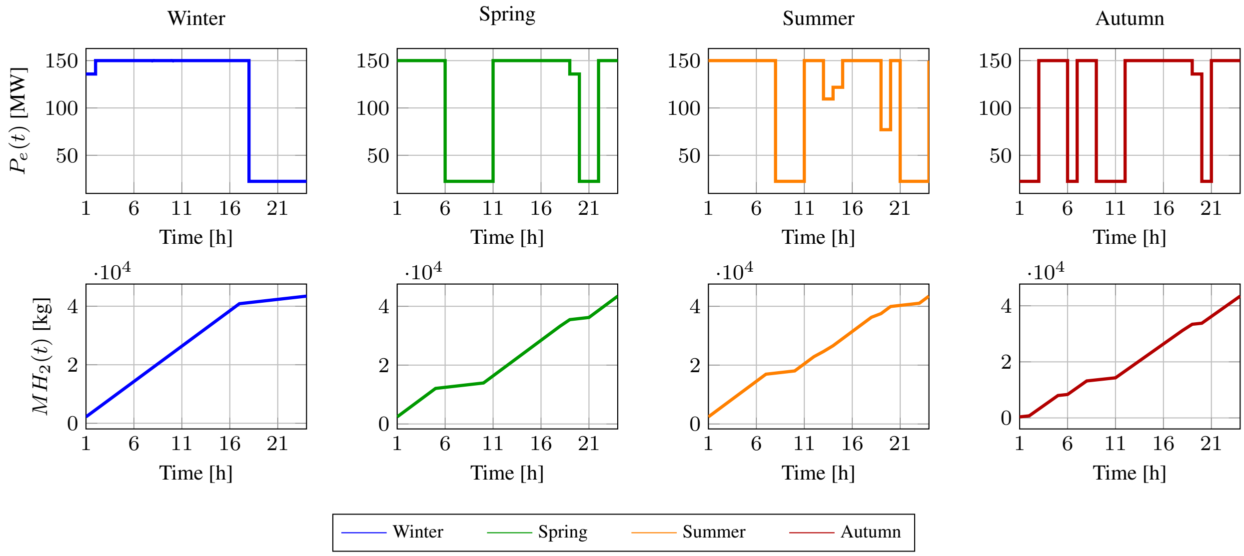

Figure 14. Hydrogen system operation across seasons: (a) Electrolyzer power $P_e(t)$ in [MW] and (b) cumulative hydrogen production $MH_2(t)$ in [kg].

5 Conclusions

This work presented a predictive nonlinear optimization framework for the operation of AC/DC energy islands, validated through a case study based on the Princess Elisabeth Energy Island. The reliability of the proposed approach was confirmed through validation with the Python-based power flow tool pyflow_acdc, developed by Valerio et al. (2025), providing a strong basis for the subsequent multiperiod and seasonal optimization analyses. The linear model for green hydrogen production, whose parameters were calculated using a measurement-based optimization approach, demonstrated significantly improved accuracy over conventional constant-efficiency models, achieving a mean modeling error below 1.5%. Seasonal analyses highlighted the flexibility and robustness of the proposed framework, which dynamically adjusts energy dispatch, BESS management, and hydrogen production to maximize economic revenues while ensuring secure operation of the energy island and the power system. The integration of BESS and hydrogen systems enabled efficient energy shifting: batteries were charged during periods of low electricity prices and discharged during peak price periods, while hydrogen systems absorbed excess renewable energy when export was less profitable, guaranteeing hydrogen production targets. Furthermore, realistic offshore wind conditions were modeled using Youwind's commercial platform, including wake effects, ensuring seasonally representative inputs. The results confirm that the proposed optimization approach effectively adapts to seasonal variability, maximizing operational efficiency and economic performance in future hybrid AC/DC energy island scenarios.

Author contributions. Mario Useche-Arteaga: Writing – review & editing, Writing – original draft, Visualization, Validation, Software, Methodology, Investigation, Formal analysis, Conceptualization. Pieter Gebraad: Data collection, Methodology, Writing review & editing, Validation, Supervision, Formal analysis. Oriol Gomis-Bellmunt: Writing – review & editing, Validation, Supervision, Project administration, Methodology. Marc Cheah-Mane: Writing – review & editing, Validation. Vinicius Lacerda: Writing – review & editing, Validation.

Competing interests. The authors declare that they have no known competing financial interests or personal relationships that could have appeared to influence the work reported in this paper.

Acknowledgements. This work has received funding from the ADOreD project of the European Union's Horizon Europe Research and Innovation program under the Marie Skłodowska-Curie grant agreement No 101073554.

https://doi.org/10.5194/wes-2025-102
Preprint. Discussion started: 2 July 2025

References

Ansari, J. A., Liu, C., and Khan, S. A.: MMC Based MTDC Grids: A Detailed Review on Issues and Challenges for Operation, Control and Protection Schemes, IEEE Access, 8, 168 154–168 165, https://doi.org/10.1109/ACCESS.2020.3023544, 2020.

Arteaga, M. U., Lacerda, V. A., Bellmunt, O. G., and Mañe, M. C.: Taking advantage of PV systems for multi-period optimal reactive power dispatch: A Convex Optimization Approach, in: 2023 IEEE PES Innovative Smart Grid Technologies Europe (ISGT EUROPE), pp. 1–5, https://doi.org/10.1109/ISGTEUROPE56780.2023.10408242, 2023.

Cao, J. and Yan, Z.: AC/DC optimal power flow problem considering wind farm integration, in: 2016 IEEE Power and Energy Society General Meeting (PESGM), pp. 1–5, https://doi.org/10.1109/PESGM.2016.7741125, 2016.

der Straeten, T. V.: Public consultation on the offshore wind tender for the Princess Elisabeth Zone, economie and Minister for Energy of Belgium, 2022.

Dozein, M. G., De Corato, A. M., and Mancarella, P.: Virtual Inertia Response and Frequency Control Ancillary Services From Hydrogen Electrolyzers, IEEE Transactions on Power Systems, 38, 2447–2459, https://doi.org/10.1109/TPWRS.2022.3181853, 2023.

Elexon: BMRS Market Index Prices, https://bmrs.elexon.co.uk/market-index-prices, contains BMRS data © Elexon Limited copyright and database right 2025, 2025.

ENTSO-E: Transparency Platform, https://newtransparency.entsoe.eu/, 2025.

Ergun, H., Dave, J., Van Hertem, D., and Geth, F.: Optimal Power Flow for AC–DC Grids: Formulation, Convex Relaxation, Linear Approximation, and Implementation, IEEE Transactions on Power Systems, 34, 2980–2990, https://doi.org/10.1109/TPWRS.2019.2897835, 2019.

Federal Public Service Economy of Belgium: Digital Database Princess Elisabeth zone, Wind Resource Assessment, https://offshore.digital-database.economie.fgov.be/#/category/59, accessed: 2023-12-20, 2024.

Garces, A.: Optimal power flow, pp. 171–193, https://doi.org/10.1002/9781119747291.ch10, 2022.

Ju, Y., Chen, C., Wu, L., and Liu, H.: General Three-Phase Linear Power Flow for Active Distribution Networks With Good Adaptability Under a Polar Coordinate System, IEEE Access, 6, 34 043–34 050, https://doi.org/10.1109/ACCESS.2018.2839641, 2018.

Katic, I., Højstrup, J., and Jensen, N. O.: A Simple Model for Cluster Efficiency, in: EWEC'86. Proceedings. Vol. 1, pp. 407–410, A. Raguzzi, Rome, european Wind Energy Association Conference and Exhibition, 7-9 October 1986, Rome, Italy, 1987.

Korompili, A., Wu, Q., and Zhao, H.: Review of VSC HVDC connection for offshore wind power integration, Renewable and Sustainable Energy Reviews, 59, 1405–1414, https://doi.org/10.1016/j.rser.2016.01.064, 2016.

Liu, F., Fredriksson, A., and Markidis, S.: A survey of HPC algorithms and frameworks for large-scale gradient-based nonlinear optimization, J. Supercomput., 78, 17 513–17 542, https://doi.org/10.1007/s11227-022-04555-8, 2022.

Lüth, A., Werner, Y., Egging-Bratseth, R., and Kazempour, J.: Electrolysis as a flexibility resource on energy islands: The case of the North Sea, Energy Policy, 185, 113 921, https://doi.org/10.1016/j.enpol.2023.113921, 2024.

Matute, G., Yusta, J., Beyza, J., and Correas, L.: Multi-state techno-economic model for optimal dispatch of grid connected hydrogen electrolysis systems operating under dynamic conditions, International Journal of Hydrogen Energy, 46, 1449–1460, https://doi.org/10.1016/j.ijhydene.2020.10.019, 2021.

Mohy-ud-din, G., Heidari, R., Ergun, H., and Geth, F.: AC–DC security-constrained optimal power flow for the Australian National Electricity Market, Electric Power Systems Research, 234, 110 784, https://doi.org/10.1016/j.epsr.2024.110784, 2024.

https://doi.org/10.5194/wes-2025-102
Preprint. Discussion started: 2 July 2025

Neuwirth, M., Fleiter, T., Manz, P., and Hofmann, R.: The future potential hydrogen demand in energy-intensive industries - a site-specific approach applied to Germany, Energy Conversion and Management, 252, 115 052, https://doi.org/10.1016/j.enconman.2021.115052, 2022.

Østergaard, J., Christensen, E., Halsnæs, K., Riisager-Simonsen, C., Lisbjerg, D., Jensen, A., Duus, J., Madsen, H., Frandsen, H., Savaghebi, M., Zhang, W., Keles, D., Ladenburg, J., Vest, M., Seger, B., Mortensen, N., Sin, G., Kitzing, L., Kolios, A., Thomsen, K., Dominkovic, D., Katsanos, E., Zania, V., Riisager, A., Astrup, T., Sulayman, A., Hoffmann, U., Andersen, D., Brückner, L., Andersen, M., and Uhd, L.: Denmark as the Energy Island Pioneer, Technical University of Denmark, 2023.

Pozo, D.: Linear battery models for power systems analysis, Electric Power Systems Research, 212, 108 565, https://doi.org/10.1016/j.epsr.2022.108565, 2022.

Raheli, E., Werner, Y., and Kazempour, J.: A conic model for electrolyzer scheduling, Computers Chemical Engineering, 179, 108 450, https://doi.org/10.1016/j.compchemeng.2023.108450, 2023.

Rodrigues, S., Restrepo, C., Kontos, E., Teixeira Pinto, R., and Bauer, P.: Trends of offshore wind projects, Renewable and Sustainable Energy Reviews, 49, 1114–1135, https://doi.org/10.1016/j.rser.2015.04.092, 2015.

Teng, Y., Wang, Z., Li, Y., Ma, Q., Hui, Q., and Li, S.: Multi-energy storage system model based on electricity heat and hydrogen coordinated optimization for power grid flexibility, CSEE Journal of Power and Energy Systems, 5, 266–274, https://doi.org/10.17775/CSEEJPES.2019.00190, 2019.

Ueckerdt, F., Verpoort, P. C., Anantharaman, R., Bauer, C., Beck, F., Longden, T., and Roussanaly, S.: On the cost competitiveness of blue and green hydrogen, Joule, 8, 104–128, https://doi.org/10.1016/j.joule.2023.12.004, 2024.

Useche-Arteaga, M. and et al.: Energy Islands: Opportunities, Challenges and Topologies, SSRN., https://doi.org/10.2139/ssrn.476187, 2024.

Useche-Arteaga, M., Gomis-Bellmunt, O., Cheah-Mane, M., Lacerda, V., and Gebraad, P.: AC energy islands for the optimal integration of offshore wind energy resources: Operation strategies using multi-objective nonlinear programming, Sustainable Energy, Grids and Networks, 40, 101 576, https://doi.org/10.1016/j.segan.2024.101576, 2024a.

Useche-Arteaga, M., Gomis-Bellmunt, O., Cheah-Mane, M., Lacerda, V., and Gebraad, P.: AC energy islands for the optimal integration of offshore wind energy resources: Operation strategies using multi-objective nonlinear programming, Sustainable Energy, Grids and Networks, 40, 101 576, https://doi.org/https: 10.1016/j.segan.2024.101576, 2024b.

Valerio, B. C., Lacerda, V. A., Cheah-Mane, M., Gebraad, P., and Gomis-Bellmunt, O.: An optimal power flow tool for AC/DC systems, applied to the analysis of the North Sea Grid for offshore wind integration, IEEE Transactions on Power Systems, pp. 1–14, https://doi.org/10.1109/TPWRS.2025.3533889, 2025.

Viaene, P., Baert, P., Ghysels, V., Remy, X., Czupper, L., and Aerts, W.: Belgian offshore wind – upcoming tendering of the Princess Elisabeth zone, Clifford Chance, 2022.

Werner, Y.: Modeling Electrolyzers and Gas Networks for Integration with Power Systems, Ph.D. thesis, Technical University of Denmark, https://doi.org/10.11581/DTU.00000301, 2023.

Williams, R. and Zhao, F.: Global Offshore Wind Report 2023, Global Wind Energy Council, 2023.

Yang, J., Chi, H., Cheng, M., Dong, M., Li, S., and Yao, H.: Performance analysis of hydrogen supply using curtailed power from a solar-wind-storage power system, Renewable Energy, 212, 1005–1019, https://doi.org/10.1016/j.renene.2023.05.094, 2023.

Youwind: Youwind Application, a web-based wind park development tool, https://app.youwindrenewables.com, 2025.

Zahle, F., Barlas, A., Lønbæk, K., Bortolotti, P., Zalkind, D., Wang, L., Labuschagne, C., Sethuraman, L., and Barter, G.: Definition of the IEA Wind 22-Megawatt Offshore Reference Wind Turbine, Technical University of Denmark, https://doi.org/10.11581/DTU.00000317, dTU Wind Energy Report E-0243 IEA Wind TCP Task 55, 2024.

https://doi.org/10.5194/wes-2025-102
Preprint. Discussion started: 2 July 2025

Øystein Ulleberg: Modeling of advanced alkaline electrolyzers: a system simulation approach, International Journal of Hydrogen Energy, 28, 21–33, https://doi.org/10.1016/S0360-3199(02)00033-2, 2003.